# Light-induced absorption changes by excitation of metastable states in $Na_2[Fe(CN)_5NO]2H_2O$ single crystals

D. Schaniel* and J. Schefer
*Laboratory for Neutron Scattering, ETHZ & PSI, CH-5232 Villigen, PSI, Switzerland*

B. Delley
*Condensed Matter Theory Group, FUN Department, PSI, CH-5232 Villigen, PSI Switzerland*

M. Imlau
*Fachbereich Physik, University of Osnabrück, D-49069 Osnabrück, Germany*

Th. Woike
*Institut für Mineralogie, University at Cologne, D-50674 Köln, Germany*
(Received 9 April 2002; published 2 August 2002)

The ground state and the light-induced metastable states of $Na_2[Fe(CN)_5NO]\cdot 2H_2O$ were investigated by polarized optical absorption spectroscopy on single crystals. An orbital level scheme is proposed for the ground state and the two metastable states SI and SII. Based on polarization analysis of the electronic transitions and density of states calculations using density functional theory (DFT), three electronic transitions were tentatively assigned to the calculated transitions of the orbital level scheme of SI and four to that of SII. Isosbestic points at 562 and 375 nm in the absorption spectra during the population of SI indicate that anions are transferred from the ground state into SI. No optical depopulation process from SI into the ground state is observed between 375 and 562 nm. An effective transfer from SI into SII can be performed by irradiation with light of wavelength above 770 or 910 nm and polarization of the light parallel to the *c* or *a* axis of the orthorhombic crystal, respectively.

DOI: 10.1103/PhysRevB.66.085103 PACS number(s): 78.40.−q, 33.20.Kf, 31.15.Ew

## I. INTRODUCTION

Light-induced metastable states are of fundamental importance for basic research and technological applications in the field of holographic information storage as well as energy storage. In long-living photoexcited molecules the electron density is adjusted to the relaxed nuclear configurations possibly combined with a change of the dipole or higher electronic moments of the whole system. This is the reason for a kind of photorefractive effect[1,2] that opens the possibility of volume holographic data storage. Concomitant with the rearranged electron density new electronic transitions appear in the near infrared and ultraviolet spectral range,[3] so that holograms can be written in this very large spectral range, yielding a modulation of the refractive index[1] of $\Delta n = 1.14 \times 10^{-3}$, which is an order of magnitude higher than in photorefractive oxides such as $BaTiO_3$.[4]

Such extremely long-living metastable states can be excited in anions or cations containing a nitrosyl-ligand N-O such as $[ML_x(NO)]^n$, *M* being a transition metal, e.g., Fe, Ni, Ru, Os, Mo, and *n* being the formal charge of the anion/cation. The ligands $L_x$ vary from atoms (F,Cl,Br,J, etc.) to complex-ligands ($CN, NH_3, NO_2$, etc.).[5–9] Compounds containing $N_2$ instead of NO as the active ligand were found recently,[10] showing that they base on a general physical effect. The fundamental and necessary electronic transition for the excitation produced by the illumination is the excitation from occupied (mainly *d*) orbitals of the central atom into the empty antibonding $\pi^*$ orbital of the active ligand ($NO, N_2$, etc.) from which a relaxation into the metastable states occurs. As a general rule we propose, that if the lifetime in the antibonding $\pi^*$ orbital is long enough, e.g, in the range of nanoseconds to microseconds, the structure relaxes into a stable configuration and the excited electron thermalizes into the long-living metastable states. Such a charge transfer transition ($d \rightarrow \pi^*$) is necessary for the formation of the metastable states. This rule is supported by calculations using density functional theory (DFT).[11–14] Up to now two metastable states SI and SII, which can be excited by irradiation with light below characteristic temperatures, are known. The maximum decay temperature of 273 K for SI was found in $[Ru(NH_3)_5NO]Cl_3$.[9] [Decay temperature should not be understood as a sharp transition temperature. It is determined by dynamic differential scanning calorimetry (DDSC) measurements and describes the temperature of the peak maximum of the heat flow and is therefore dependent on the heating rate. The decay follows an Arrhenius law.] $Na_2[Fe(CN)_5NO]\cdot 2H_2O$ (SNP) is the most investigated system and the up to now obtained experimental and theoretical results are covered by two recent review articles.[15,16] In SNP the decay temperatures of SI and SII are lying at about 198 and 147 K, respectively. These states are separated from the ground state by potential barriers of 0.7 eV (SI) and 0.5 eV (SII).[17] They can be excited by irradiation with light in the spectral range of 350–580 nm. The maximum of about 50% of the $[Fe(CN)_5NO]^{2-}$ anions can be transferred into SI using a light polarization perpendicular to the quasifourfold N-C-Fe-N-O axis and a wavelength between 440 and 470 nm. Deexcitation into the ground state takes place by illumination with light in the spectral range of 600–1200 nm or by increasing the temperature to overcome the potential barriers. Illumination with light in the region of 900–1200

 ©2002 The American Physical Society

nm below the decay temperature of SII transfers about 30–35 % of the anions from SI into SII and the rest into the ground state.[18] Irradiation with light excites the electrons from the GS into the $\pi^*$(NO) orbital. These ''hot'' electrons relax into the minimum of the $\pi^*$(NO) potential. At the crossing point of the potentials of GS and SI the relaxation back into GS or into SI occurs together with the thermalization process, since no luminescence is observed in the spectral range of 300–3000 nm. The high potential barrier of 0.7 eV (SI) and of 0.5 eV (SII) causes the stability of SI/SII at sufficiently low temperatures. The irradiation of SI in the range of 600–1200 nm leads again to the excitation of the $\pi^*$(NO) orbital, from which a relaxation into GS or into SII occurs, as detected and discussed below. The four-level system GS, $\pi^*$(NO), SI, SII (for illustration see Fig. 2 in Ref. 19) explains the population, depopulation, and transfer between GS, SI, and SII completely.

The new states SI, SII are lying energetically about 1 eV above the ground state.[18] From the structural point of view there are two different results: Neutron diffraction proposed that only the Fe-N and N-O bond distances are elongated by a small amount[20,21] whereas x-ray diffraction proposed an inversion of the N-O ligand to Fe-O-N for SI and a 90° rotation of the N-O ligand for SII,[9,22] so that the reaction coordinates for the two excitations are either the rotation angle $\phi_{SI}=180°$ from Fe-N-O to the inverted Fe-O-N (SI) or the rotation angle $\phi_{SII}=90°$ from Fe-N-O to the bent configuration Fe-(NO). For SI the quasi-$C_{4v}$ $(4m)$ symmetry of the $[Fe(CN)_5NO]^{2-}$ anions is conserved, whereas for SII it is reduced to $C_s$ $(m)$, thereby lifting all degeneracies of vibrational bands and electronic orbitals. This can be detected by vibrational or polarized absorption spectroscopy, which is the topic of this paper.

We performed polarized absorption spectroscopic measurements in order to determine the symmetry and the energetic positions of the electronic transitions of the ground state and the two metastable states SI and SII of $Na_2[Fe(CN)_5NO]\cdot 2H_2O$. We present the orbital-level diagrams of the ground state and the two excited states and construct a potential-energy scheme on the basis of DFT calculations using the N-O-inversion for SI and the bent configuration for SII. From the area of the absorption bands we further get a first view inside the lifetimes of the charges excited into the $\pi^*$(NO) and the energetically higher orbitals.

## II. EXPERIMENTAL AND THEORETICAL DETAILS

Single crystals of orthorhombic sodium nitroprusside (SNP) $Na_2[Fe(CN)_5NO]\cdot 2H_2O$, space group $Pnnm$, four molecules per unit cell,[23,24] were grown from aqueous solution and cut perpendicular to the crystallographic axes. Specimens of dimension 20 mm×10 mm were ground to thicknesses between 0.5 and 0.04 mm using a mixture of $Al_2O_3$ and propanol and finally etched with a mixture of water and propanol. They were mounted on a sample holder diving into a nitrogen-filled quartz Dewar. The temperature is kept constant at 100 K. The expanded beam of an $Ar^+$ laser (λ=476.5 nm) strikes the sample perpendicular to the entrance face with an intensity of $I_L=80$ mW/cm$^2$. In order

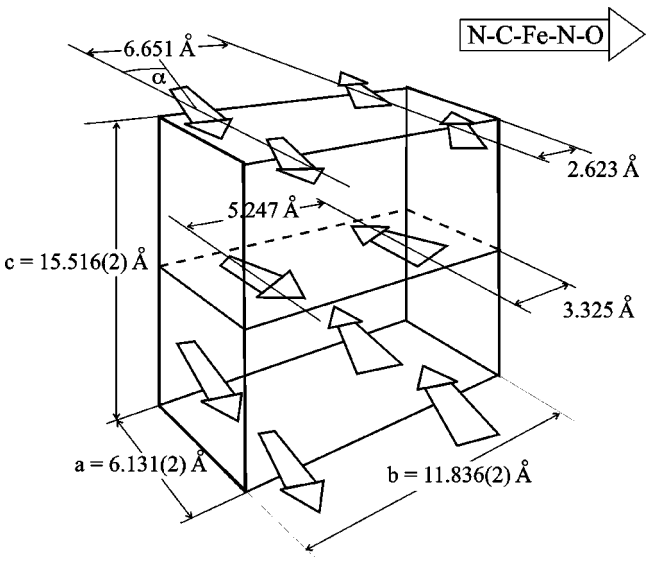


FIG. 1. Unit cell of SNP. Arrows indicate the direction of the quasifourfold axis N-C-Fe-N-O of the anion ($\alpha$=37.2°).

to reach the maximum population of 50% of the metastable state SI a total exposure of about $Q=I_L\cdot t=2800$ W s/cm$^2$ (for a sample of 0.25 mm thickness) is needed and the laser beam has to be polarized parallel to the *c* axis of the crystal, perpendicular to the quasifourfold (N-C-Fe-N-O) axis of the anion (see Fig. 1). The absorption spectra were measured with a two beam spectrophotometer (Perkin-Elmer) equipped with a Glan-Thompson polarizer and a quartz Dewar. The wavelength resolution was 4 nm over the whole spectral range of 220–1200 nm. The spectra were deconvoluted by fitting a sum of Gaussian curves to the corresponding electronic transitions together with a horizontal baseline, since we have not made any corrections of the transmission by the reflection given by the refractive indices.

Irradiation with a wavelength of λ=476.5 nm produces simultaneously about 2% of SII and about 45% of SI. By heating the crystal to $T=150$ K, SII can be completely depopulated so that only absorption caused by GS and SI is measured. The transfer of SI into SII can be performed by irradiation with light of the wavelength λ=1064 nm.[18] With an exposure of $Q=250$ W s/cm$^2$ the maximum population of about 35% of SII is reached and SI is completely depopulated, so that only GS and SII are present. As evidenced by isosbestic points (points where the absorption coefficient $\alpha$ is independent of the population of the different states) in the blue, red,[25] and infrared spectral range (see below), the population of SI and SII results in a decrease of the number density $n_{GS}$ of the anions in the ground state so that there exists a spectral region, where only the behavior of the ground state can be detected. The population $P(Q)$, e.g., of SI, is given by the ratio of the number density of the anions

$$P(Q)=\frac{n_{SI}(Q)}{n_{tot}} \tag{1}$$

and depends on the exposure $Q=I_L\cdot t$, given by the product of constant light intensity $I_L$ and irradiation time *t*. The total

density of anions $n_{tot}$ must be constant

$$n_{tot}=n_{GS}+n_{SI}=\text{const.} \tag{2}$$

At Q=0, $n_{tot}$ is the number density in the ground state

$$n_{tot}=n_{GS}(Q=0) \tag{3}$$

known from the structure[24] as $n_{tot}=Z/V_{\text{unit cell}}=3.5\times10^{21}\text{cm}^{-3}$. Therefore

$$P(Q)=\frac{n_{tot}-n_{GS}}{n_{tot}}=\frac{n_{GS}(Q=0)-n_{GS}(Q)}{n_{GS}(Q=0)}. \tag{4}$$

By measuring the absorption coefficient $\alpha$ in the spectral region where only the ground state is present:

$$\alpha_{GS}(Q)=n_{GS}(Q)\cdot\sigma(\lambda), \tag{5}$$

whereby $\sigma(\lambda)$ is the wavelength-dependent cross-section, the population can be determined as a function of exposure by

$$P(Q)=\frac{\alpha_{GS}(Q=0)-\alpha_{GS}(Q)}{\alpha_{GS}(Q=0)}. \tag{6}$$

With this information the deconvolution of the decreased absorption bands of the ground state and the bands of SI or SII is straightforward.

The measured spectra are evaluated by fitting Gaussian functions on every absorption band. Neglecting the almost isotropic refractive indices,[2] we can estimate the lifetime of excited charges in the $\pi^*$(NO) and the energetically higher orbitals, using[26]

$$A_{21}=\frac{1}{\tau_{21}}=\frac{8\pi c}{n_i}\frac{g_1}{g_2}\tilde{\nu}_{21}^2\int\alpha(\tilde{\nu})d\tilde{\nu}. \tag{7}$$

$n_i$ ($i$=GS,SI,SII) is the number density of the anions, $\tilde{\nu}_{21}=\tilde{\nu}_{12}$ is the wavenumber at the maximum of the absorption band, $c$ is the velocity of light, $\int\alpha(\tilde{\nu})d\tilde{\nu}$ is the integral over the measured absorption coefficient (Gaussian band), $\tilde{\nu}$ is the wave number in $\text{cm}^{-1}$, and $g_1, g_2$ are the degeneracies of the starting and excited state, respectively. A sum of Gaussian bands is fitted to the wave number dependent absorption coefficient $\alpha(\tilde{\nu})$:

$$\alpha(\tilde{\nu})=\sum_{i=1}^{n}\alpha(\tilde{\nu})_{\text{max},i}\exp\left[-\ln 2\frac{(\tilde{\nu}-\tilde{\nu}_{\text{max},i})^2}{\Gamma_i^2}\right], \tag{8}$$

where $\alpha(\tilde{\nu})_{\text{max},i}$ is the maximum of the $i$th absorption band and $\Gamma_i$ is the full width at half maximum (FWHM) of the $i$th band. The spontaneous transition probability $A_{21}$ is connected with the oscillator strength $f_{21}$ by

$$f_{21}=\frac{mc}{8\pi^2e^2}\frac{1}{\tilde{\nu}_{21}^2}A_{21}=\frac{mc^2}{\pi e^2 n_i}\frac{g_1}{g_2}\int\alpha(\tilde{\nu})d\tilde{\nu}, \tag{9}$$

where $m$ and $e$ are the electron mass and charge, respectively. The assignments of the measured transitions are based on polarization analysis of each observed transition and on calculations of the total and partial density of states, using density functional theory (DFT). For the polarization analysis we make use of elementary symmetry arguments. The nitrosyl-anions are lying with their quasifourfold axis (N-C-Fe-N-O) in antiparallel couples in the $a$-$b$ plane of the unit cell as shown in Fig. 1. The angle $\alpha$ between the C-Fe direction and the $a$ axis is 37.2°. Other angles are $\angle$(Fe-N,$a$ axis)=34.0° and $\angle$(Fe-O,$a$ axis)=32.4°.[21] As the $c$ axis is perpendicular to the N-C-Fe-N-O axis, light with the electric field vector parallel to the $c$ axis represents a special polarization direction. Under $4m(C_{4v})$ symmetry allowed electronic transitions occur for $\mathbf{E}\|c$ axis as $e$ symmetry and for $\mathbf{E}\|$(Fe-N-O) as $a_1$ symmetry. Using the same notation as in earlier DFT calculations[11] for the ground state, the following transitions are symmetry allowed: $2b_2\rightarrow7e(\mathbf{E}\|c)$, $6e\rightarrow7e(\mathbf{E}\|$Fe-N-O), $6e\rightarrow3b_1(\mathbf{E}\|c)$ and $6e\rightarrow5a_1(\mathbf{E}\|c)$. The transitions $2b_2\rightarrow3b_1$ and $2b_2\rightarrow5a_1$ are dipole forbidden, but vibrationally allowed when coupling to modes with corresponding symmetry.

The density of states (DOS) and the partial density of states (PDOS) were calculated for the SNP crystal in GS, SI, and SII conformation using the *DMOL*$^3$ density functional method.[11,27,28] An inversion of the N-O bond for SI and a 90°-bent configuration for SII was assumed as proposed by Carducci *et al.*[22] in order to have well defined potential minima by the defined structure and to compare the calculated results with our measurements. The BP functional[29,30] was used. Integration in $k$-space was done with an unshifted 4 4 4 mesh, and the PDOS was calculated from the Mulliken analysis with the tetrahedron integration method. The PDOS gives information about the orbital character and overlap as a rough estimate of the matrix elements, yielding therefore information about the observability of the transitions. The energy separations are first order estimates for the excitation energies, whereby the final state electronic relaxation is neglected.

## III. EXPERIMENTAL RESULTS

### A. Transitions of the ground state

The electronic absorption spectra of SNP in the ground state are needed for the comparison with those of the metastable states and for the explicit assignment to the group theoretical considerations. Absorption spectra of a solution of SNP in water at room temperature are presented in Refs. 31 and 32. These spectra exhibit all the possible transitions which can be resolved and detected over the whole spectral range at room temperature. First polarized absorption spectra of single crystals were measured by Manoharan and Gray.[33] We have measured polarized absorption spectra of single crystals of SNP as shown in Fig. 2 at room temperature as well as at $T=100$ K. All absorption bands are polarized. Due

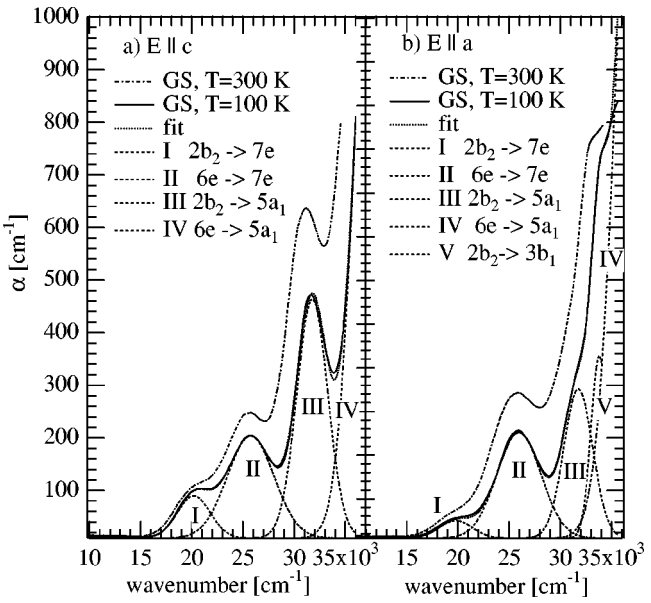


FIG. 2. Transitions of GS in single crystals of SNP (a) $\mathbf{E}\|c$, (b) $\mathbf{E}\|a$.

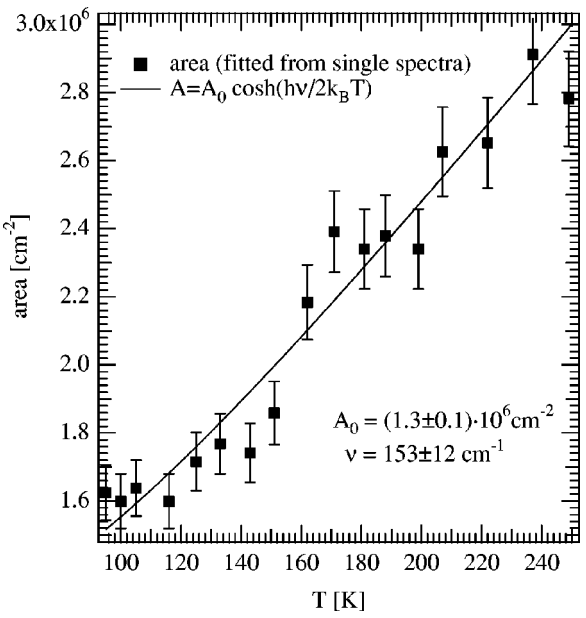


FIG. 3. Temperature dependence of the area of the $2b_2 \rightarrow 5a_1$ transition in GS of SNP.

to the strong absorption in the UV region, transitions at higher energies than 4.5 eV were not detected. The preparation of single crystals is limited to a minimum of 40 $\mu$m thickness. In Table I we present the refined parameters (position $\tilde{\nu}_{\max}$, FWHM $\Gamma$, and area $A$) of the observed transitions using the polarization of the probing light along the $c$ or $a$ axis of the crystal. Further, using Eqs. (7) and (9), the lifetime $\tau$ of the excited states and the oscillator strength $f$ can be determined, knowing the degeneracies $g_{1,2}$. Our assignments are given in the first column. The observed transition energies $\tilde{\nu}_{\max}^{\exp}$[eV] are compared to the calculated energy differences $\tilde{\nu}_{\max}^{\text{calc}}$ in the last two columns. The transition at about 20 000 $\text{cm}^{-1}$ is twice as strong for $\mathbf{E}\|c$ compared to $\mathbf{E}\|a$, therefore we assign it to the $2b_2 \rightarrow 7e$ transition which is symmetry allowed perpendicular to the fourfold axis of the molecule. The second transition at about 26 000 $\text{cm}^{-1}$ is slightly stronger for $\mathbf{E}\|a$. We assign it to $6e \rightarrow 7e$, being much broader than the first transition. The third transition at about 31 700 $\text{cm}^{-1}$ is narrower and shows a distinct temperature dependence of its position and size. We assign it therefore to the vibrationally allowed transition $2b_2 \rightarrow 5a_1$. As the phonons freeze in with decreasing temperature the absorption strength of this band decreases. In order to underline the assignment of the $2b_2 \rightarrow 5a_1$ transition we have measured the temperature dependence of its intensity (area), as shown in Fig. 3. Fitting a simple Debye behavior

$$A = A_0 \cosh\left(\frac{h\tilde{\nu}}{2k_B T}\right) \tag{10}$$

to the given temperature dependence, a wave number of $\tilde{\nu} = 153 \pm 12$ $\text{cm}^{-1}$ is obtained, which is in agreement with the wave numbers of the $\tilde{\delta}$(C-Fe-N) and $\tilde{\delta}$(C-Fe-C) deformation modes with $e$ symmetry.[34] We know from the spectrum measured on a solution of SNP that the fourth band is lying

TABLE I. Refined parameters to the absorption spectra of GS in single crystals of SNP at $T = 100$ K.

| $\|c$ | $\tilde{\nu}_{\max}$[$\text{cm}^{-1}$] | A [$10^6\text{cm}^{-2}$] | $\Gamma$[$\text{cm}^{-1}$] | $\tau$[$\mu$s] | f [$10^{-3}$] | $\tilde{\nu}_{\max}^{\exp}$[eV] | $\tilde{\nu}_{\max}^{\text{calc}}$[eV] |
|---|---|---|---|---|---|---|---|
| $2b_2 \rightarrow 7e$ | 20196±80 | 0.32±0.02 | 3775±100 | 72 | 0.051 | 2.50 | 2.204 |
| $6e \rightarrow 7e$ | 25753±100 | 1.12±0.04 | 5380±200 | 6.3 | 0.36 | 3.19 | 2.638 |
| $2b_2 \rightarrow 5a_1$ | 31776±100 | 1.72±0.08 | 3560±100 | 2.7 | 0.55 | 3.94 | 4.156 |
| $6e \rightarrow 5a_1$ | 37700±100 | 5.5±0.5 | 4220±300 | 0.30 | 1.8 | 4.67 | 4.59 |
| $\|a$ | $\tilde{\nu}_{\max}$[$\text{cm}^{-1}$] | $A$[$10^6\text{cm}^{-2}$] | $\Gamma$[$\text{cm}^{-1}$] | $\tau$[$\mu$s] | f [$10^{-3}$] | $\tilde{\nu}_{\max}^{\exp}$[eV] | $\tilde{\nu}_{\max}^{\text{calc}}$[eV] |
| $2b_2 \rightarrow 7e$ | 19792±80 | 0.16±0.01 | 3745±100 | 150 | 0.026 | 2.45 | 2.204 |
| $6e \rightarrow 7e$ | 25956±100 | 1.30±0.04 | 5060±200 | 5.4 | 0.42 | 3.22 | 2.638 |
| $2b_2 \rightarrow 5a_1$ | 31754±100 | 1.21±0.08 | 3330±100 | 3.8 | 0.39 | 3.94 | 4.156 |
| $2b_2 \rightarrow 3b_1$ | 33800±100 | 0.84±0.06 | 1900±100 | 4.9 | 0.27 | 4.19 | 4.799 |
| $6e \rightarrow 5a_1$ | 37600 | 9.5±0.8 | 4700±300 | 0.17 | 16.1 | 4.66 | 4.59 |

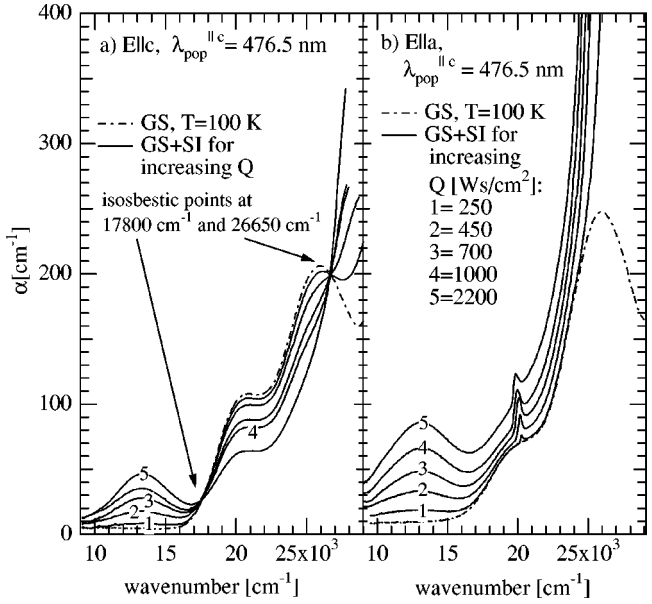


FIG. 4. $Q$ dependence of the transitions of GS and SI in the visible and near infrared spectral range. (a) $\mathbf{E}\|c$, (b) $\mathbf{E}\|a$.

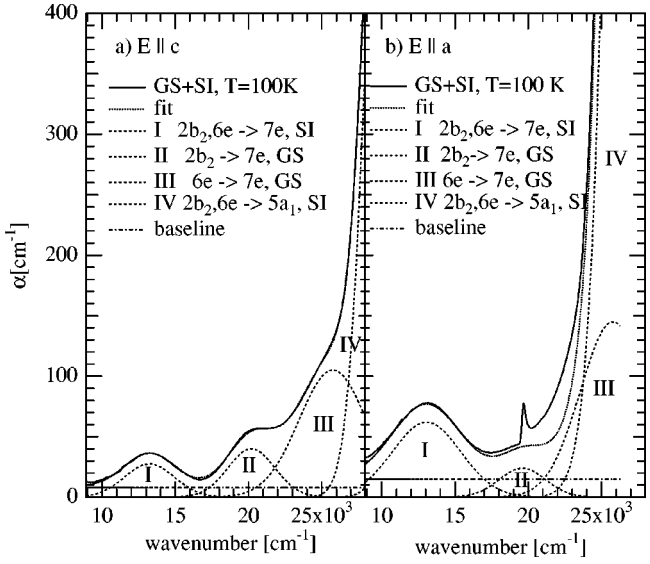


FIG. 5. Deconvolution of the spectra of GS and SI in SNP. (a) $\mathbf{E}\|c$, (b) $\mathbf{E}\|a$.

approximately at 37 700 cm$^{-1}$. We therefore fitted the measured part of this absorption band using constraints for its position, thereby getting the presented result. We tentatively assign it to the $6e \rightarrow 5a_1$ transition. In the measurements with $\mathbf{E}\|a$ one further narrow transition is observed as a shoulder in the fourth absorption band. We can assign it to the $2b_2 \rightarrow 3b_1$ (dipole forbidden), because it is narrower than all other transitions and also exhibits a strong temperature dependence.

### B. Transitions of the metastable state SI

For the assignment of the new electronic transitions and for the understanding of the metastable states it is important to detect the decrease of the absorption bands of GS and the increase of new absorption bands while populating the single crystals. In Fig. 4 the absorption spectra for different exposures $Q$ are shown. The crystal thickness was 0.06 mm. After every irradiation cycle the crystal was heated to 150 K in order to eliminate SII, therefore only GS and SI are present. For the measurement with the polarization of the probing light $\mathbf{E}\|c$ [Fig. 4(a)] we observe two characteristic isosbestic points at 17 800 cm$^{-1}$ and 26 650 cm$^{-1}$. Within this interval the absorption bands of GS decrease, whereas at lower and higher wave numbers the new bands of SI appear. Clearly we can assign the new band at 13 000 cm$^{-1}$ to SI. As explained above the existence of the isosbestic points allows us to determine the population of SI directly from the absorption spectrum by using Eq. (6). No wavelength shift of the absorption bands can occur, only the area of the bands can be changed. Figure 5(a) shows the absorption spectrum at $Q = 2500$ W s/cm$^2$ measured $\|c$ and its deconvolution. The population of SI=45% was determined using Eq. (6). Therefore the areas of the GS transitions were fixed at 55% of the values given in Table I for the deconvolution. No further absorption bands could be observed at wavenumbers below 9000 cm$^{-1}$.

The analysis of the spectra measured with light polarization along the $a$ or $b$ axis is more involved. As presented by Imlau *et al.*[35] holographic gratings are written by irradiation with only one laser beam (i.e., without a reference beam), which can be read with light polarization along the $a$ or $b$ axis. This effect is of technical interest, but has also to be taken into account when analyzing our data. Reading these gratings means that the incoming light is diffracted around the primary beam, which is detected by the spectrometer as an additional extinction, because the diffracted light misses the area of the photomultiplier. As can be seen from Fig. 4(b), in addition to the characteristic decrease and increase of the absorption bands of GS and SI, the baseline increases over the whole spectral range and a narrow extinction band arises at $\tilde{\nu} = 20\,267$ cm$^{-1}$ and shifts to $\tilde{\nu} = 19\,914$ cm$^{-1}$ during the population of SI. A systematic study of this extinction, which is characteristic for reading holographic gratings, will be presented elsewhere.[36] We use its shift to determine the population of SI, because the decrease of GS is too much influenced by the increasing baseline, which is also produced by the holographic light scattering. For the deconvolution of the spectra, shown for a population of 40% in Fig. 5(b) (a new crystal with a different population of SI was used for the measurement with $\mathbf{E}\|a$), we have chosen a horizontal baseline. The fit deviates from the measured spectrum in the range of the narrow extinction band and the strong UV bands. We assume that the holographic light scattering is more pronounced as we have considered by describing it with a constant baseline. The narrow extinction band shows an asymmetric behavior on its high-energy side, which is a clear indication for the existence of further scattering contributions. Further the very strong increase of the absorption above 22 000 cm$^{-1}$, compared to the measurement with $\mathbf{E}\|c$ axis, prevents a more precise fit to the data in this spectral

TABLE II. Refined parameters to the absorption spectra of SI in single crystals of SNP at $T=100$ K.

| $\|c$ | $\nu_{max}[cm^{-1}]$ | $A[10^6 cm^{-2}]$ | $\Gamma[cm^{-1}]$ | $\tau[\mu s]$ | f $[10^{-3}]$ | $\tilde{\nu}^{exp}_{max}$[eV] | $\tilde{\nu}^{calc}_{max}$[eV] |
|---|---|---|---|---|---|---|---|
| $2b_2,6e\rightarrow 7e$ | 13230±80 | 0.16±0.01 [a] | 4288±100 | 75 | 0.12 | 1.64 | 1.257,1.734 |
| $2b_2,6e\rightarrow 5a_1$ | 30900±500 | 0.63±0.05 [c] | 3600±500 | 0.23 | 6.7 | 3.83 | 3.815,4.292 |
| $2b_2,6e\rightarrow 3b_1$ | 35200±500 | 0.61±0.05 [c] | 4300±500 | 0.09 | 13 | 4.36 | 4.823,5.300 |
| $\|a$ | $\nu_{max}[cm^{-1}]$ | $A[10^6 cm^{-2}]$ | $\Gamma[cm^{-1}]$ | $\tau[\mu s]$ | f $[10^{-3}]$ | $\tilde{\nu}^{exp}_{max}$[eV] | $\tilde{\nu}^{calc}_{max}$[eV] |
| $2b_2,6e\rightarrow 7e$ | 13050±80 | 0.36±0.02 [b] | 5490±100 | 31 | 0.28 | 1.62 | 1.257,1.734 |
| $2b_2,6e\rightarrow 5a_1$ | 29300±500 | 0.73±0.05 [d] | 3400±500 | 0.15 | 12 | 3.63 | 3.815,4.292 |
| $2b_2,6e\rightarrow 3b_1$ | 32000±500 | 0.73±0.05 [d] | 3000±500 | 0.06 | 23 | 3.97 | 4.823,5.300 |

[a]45%.
[b]40%.
[c]3%.
[d]2% population.

range. We have therefore used the known bands from the ground state, weighted by their population of 60%, and one new band for SI as indicated in Fig. 5(b). In this spectral range an absorption of amplitude 20 $cm^{-1}$ remains unassigned. The refined parameters for the transition of SI are summarized in Table II.

Figure 6 shows the absorption spectra in the UV region. Here it is impossible to measure the spectra in the fully populated crystals as the absorption is too strong. Therefore, we measured again the increase of SI as a function of the exposure $Q$, whereby at every cycle SII was depopulated by heating to 150 K. For the measurement with polarization $\mathbf{E}\|c$ [Fig. 6(a)] we find again the isosbestic point at 26 650 $cm^{-1}$ whereas for the measurements with $\mathbf{E}\|a$ the appearance of holographic light scattering complicates the analysis of the spectra. Nevertheless for both polarizations two new absorption bands can be found by looking at the differences between consecutive spectra. Figure 7(a) shows the deconvolution of SI at an exposure of $Q=126$ W s/$cm^2$ for $\mathbf{E}\|c$. Using Eq. (6) we determined the population of SI as 3%. Therefore we subtracted the GS, weighted by 97%, from the experimentally observed spectrum, thereby obtaining the presented difference spectrum [Fig. 7(b)]. This figure shows the deconvolution of the difference spectrum of SI measured with $\mathbf{E}\|a$ and a population of 2%. The population $P$ was determined from the exposure $Q$ [as we have determined the $P(Q)$ dependence for the spectra in Fig. 4(b) from the shift of the narrow extinction band]. The refined parameters for SI in the UV regime are summarized in Table II. The final assignment of the transitions, which are indicated in Table II, will be made in the discussion and are based on the DFT calculations.

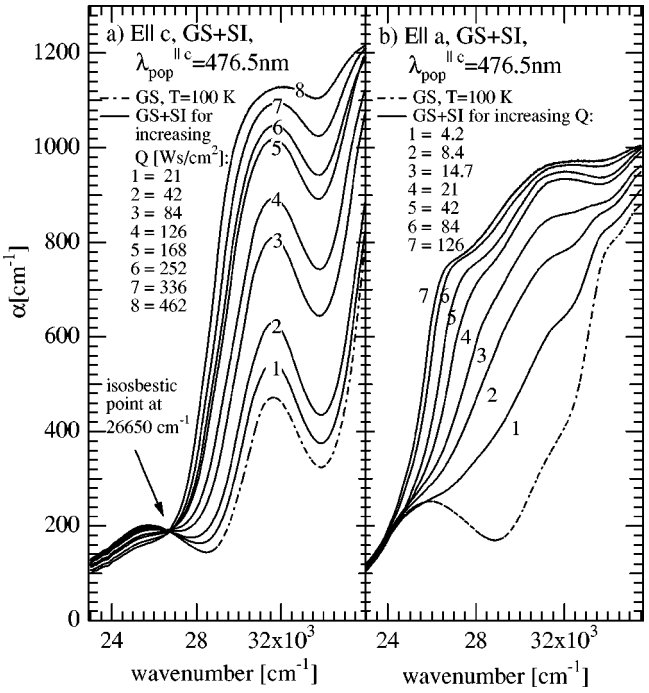


FIG. 6. $Q$ dependence of the transitions of GS and SI in the ultraviolet spectral range. (a) $\mathbf{E}\|c$, (b) $\mathbf{E}\|a$.

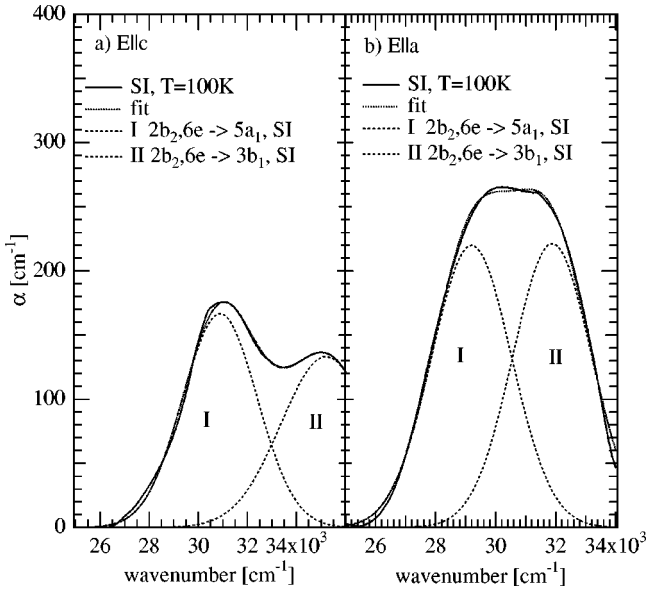


FIG. 7. Deconvolution of the spectra of SI in the ultraviolet spectral range, obtained by subtracting the contribution of GS. (a) $\mathbf{E}\|c$, (b) $\mathbf{E}\|a$.

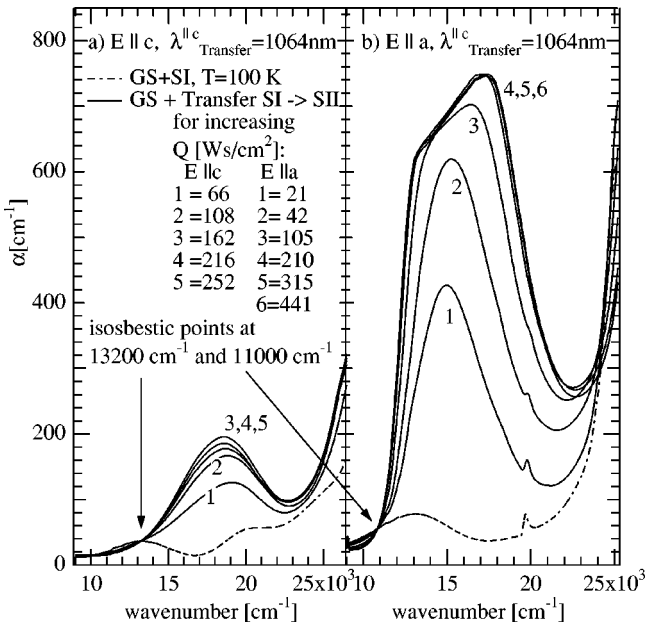


FIG. 8. $Q$ dependence of the transitions of GS, SI, and SII in the visible and near infrared spectral range during the transfer SI $\rightarrow$SII. (a) $\mathbf{E}\|c$, (b) $\mathbf{E}\|a$.

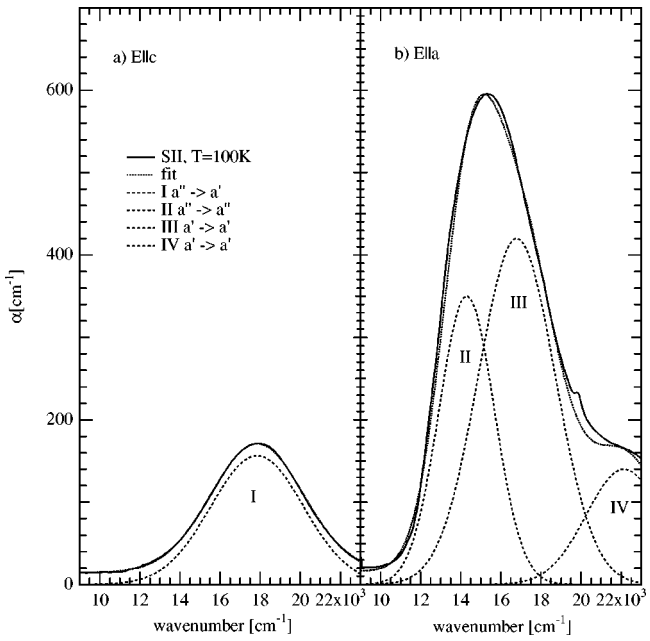


FIG. 9. Deconvolution of the transitions of SII in SNP. (a) $\mathbf{E}\|c$, (b) $\mathbf{E}\|a$.

### C. Transitions of the metastable state SII

SI can be partially transferred into SII by irradiation with light of wavelength $\lambda = 1064$ nm.[18] With this technique a maximum population of about 35% of SII is reached. Figure 8 shows the development of the spectra during the transfer SI$\rightarrow$SII, when irradiating with $\mathbf{E}\|c$ and $\lambda = 1064$ nm. Due to the increase of SII and the decrease of SI an isosbestic point appears in the near infrared region (at 13 200 $cm^{-1}$ for $\mathbf{E}\|c$ and at 11 000 $cm^{-1}$ for $\mathbf{E}\|a$) which again demonstrates the change of the number density of absorbing anions. There is no isosbestic point in the visible or UV region. This is due to the fact that in the near infrared only two states (SI and SII) contribute to the absorption. In the visible and UV the mixing of the three states GS, SI, and SII, which all change their absorption behavior, prevents the existence of isosbestic points. The deconvolution for $\mathbf{E}\|c$ is straightforward. Figure 9(a) shows the deconvoluted difference spectrum of SII (weighted GS subtracted) at $Q = 252$ $Ws/cm^2$, corresponding to a population of 38%. The band on the high energy side of the measured spectra was not refined, but a Gaussian was adapted to the curve in order to estimate its influence on the area of the refined Gaussian at 17 850 $cm^{-1}$. It turned out to be small, as shown in Fig. 9(a).

The absorption behavior for $\mathbf{E}\|a$ has again a more complicated structure. It starts with the increase of a broad absorption band, fitted by two Gaussians. A third transition appears in the region between the small extinction band of SI and the steep slope, caused by the strong bands in the UV, which could not be measured. After a certain population of SII is reached, a broad plateau builds up between 13 000 $cm^{-1}$ and 18 000 $cm^{-1}$ when further irradiating with $\lambda = 1064$ nm. At the exposure where SI is completely depopulated, indicated by the disappearance of the small extinction band at 19 900 $cm^{-1}$, this plateau reaches a maximum and decreases afterwards. At an exposure of about $Q = 2400$ $W\,s/cm^2$ it vanishes and the broad absorption band, which is present in the beginning of the transfer SI$\rightarrow$SII, is reestablished. The origin of this plateau is not understood yet. Therefore, we fitted two Gaussians to the difference spectrum at $Q = 42$ $W\,s/cm^2$ (corresponding to 27% population of SII), shown in Fig. 9(b). The difference spectrum was obtained by subtracting the weighted contributions of SI (8%) and GS (65%) as described earlier. The two bands at 14 000 and 16 400 $cm^{-1}$ are almost independent of this subtraction as the bands of GS and SI do not contribute much in this spectral region. The area of the band at 22 200 $cm^{-1}$ depends on the accuracy with which the amount of GS is determined, therefore the error made in the determination of the area is larger than for the other bands. As for the measurement with $\mathbf{E}\|c$ the influence of the energetically higher bands was taken into account, by adapting one Gaussian to the slope on the high-energy side of the spectrum. Its influence on the fitted area of the band at 22 200 $cm^{-1}$ is of the same order as the error made by the subtraction of GS, due to the fact that the slope is very steep and the overlap therefore very small. Consequently the existence of this band may be questioned. Near the small extinction band, the fit to the data was not improved, because we do not know the exact form of this band, as mentioned earlier. All in all the absorption bands of SII in the red and near infrared region are much stronger than those of SI.

## IV. DISCUSSION

Since the seminal calculations and absorption spectroscopic measurements on SNP of Manoharan and Gray,[33] later by Fenske and DeKock,[37] and Braga *et al.*[38] the possible electronic transitions of the ground state are known. However, the density functional theory provides nowadays a use-

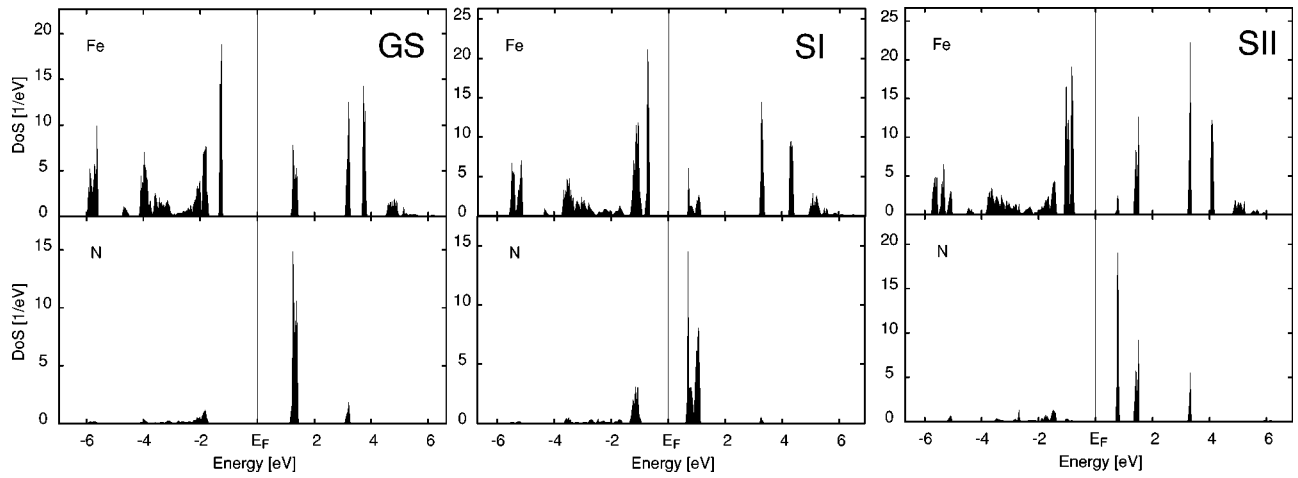


FIG. 10. Partial density of states (PDOS) for Fe and N (of N-O) for the three different states GS, SI, and SII.

ful tool to determine the orbital level ordering and energetic positions.[11] Under $C_{4v}$ symmetry (GS,SI) we obtain the energetic level ordering: $6e<2b_2<7e<5a_1<3b_1$ in which the $a_1$ and $b_1$ levels are interchanged with respect to the earlier calculations.[33,37,38] Following the proposal of Carducci *et al.*,[22] SI is characterized by an 180° inversion of the nitrosyl ligand as Fe-O-N with $C_{4v}$ symmetry and SII has a 90°-bent NO-ligand with $C_s$ symmetry, in which all degenerate levels are split into $a'$ and $a''$. Nevertheless it is not enough to know the energy levels for the assignment of the measured polarized absorption bands to corresponding transitions. But from the PDOS of GS, SI, and SII for Fe,N,O,$C_{ax}$,$N_{ax}$,$C_{eq}$,$N_{eq}$ it becomes apparent that the starting levels for the measured transitions are lying at the central Fe atom and the unoccupied levels are contributions of the Fe, N, and O (Fe-N-O). In Fig. 10 the PDOS over Fe and N are presented for GS, SI, and SII. The highest PDOS in the experimentally available energy range are lying at the Fe, N, and O atoms so that we are starting with our assignments from the HOMO of the $3d$ levels $(6e,2b_2)$. In Fig. 11 we plot the calculated orbital level scheme (Kohn-Sham eigenvalues as energies) together with the observed transitions and their experimentally determined energy (zero energy is set to the Fermi level as in Fig. 10). The assignment and level ordering of GS corresponds to that already suggested by Manoharan and Gray,[33] except for the interchange of $5a_1$ and $3b_1$. For SI, $7e$ lowers its energy whereas $2b_2$ and $6e$ increase slightly, leading to a redshift of this two transitions in the calculation. This redshift is observed experimentally, but only one transition could be found. No transition is observed below 9000 $cm^{-1}$ and no other transition of SI is allowed between 17 800 and 16 650 $cm^{-1}$ as indicated by the isosbestic points. The polarization analysis of the transition at 13 000 $cm^{-1}$ shows that it is about twice as strong when measured with $\mathbf{E}\|a$ compared to $\mathbf{E}\|c$. Since in SI $C_{4v}$ symmetry of the $[Fe(CN)_5NO]^{2-}$ anion is conserved, this must be the $6e\rightarrow 7e$ transition, because the $2b_2\rightarrow 7e$ is stronger for $\mathbf{E}\|c$, as seen in GS. This may have two reasons: either the two levels $2b_2$ and $6e$ are coincidentally degenerate, or we observe for the two different polarization directions two different transitions, i.e., for $\mathbf{E}\|c$ the $2b_2\rightarrow 7e$ and for $\mathbf{E}\|a$ the $6e\rightarrow 7e$ transition. In the second case the two levels $2b_2$ and $6e$ are again almost degenerate. In both cases the antibonding $2b_2$ orbital should not shift and the shift of the $6e$ orbital should be stronger by about 0.4 eV, which is in the range of uncorrected Kohn-Sham Eigenvalues. Nevertheless, if we try to fit the experimentally observed absorption band with two transitions, we can estimate their maximal difference in energy to be about 0.04 eV.

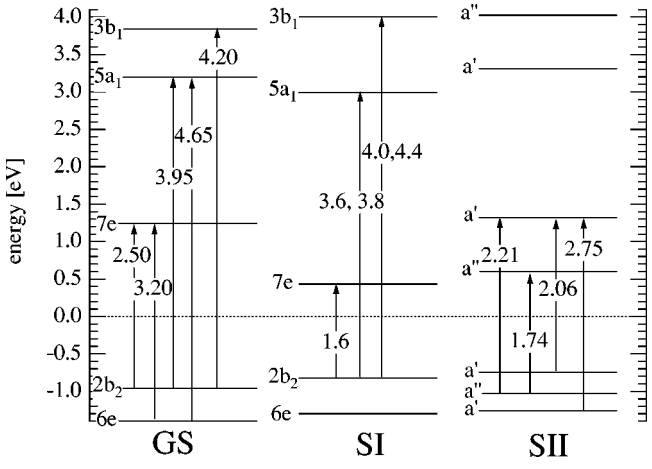


FIG. 11. Calculated orbital level diagram for GS, SI, and SII. Arrows indicate the observed transition and their experimentally determined energy.

The energy of the two transitions of SI observed in the UV roughly matches the calculated energy differences of the $(6e,2b_2)\rightarrow 5a_1$ and $(6e,2b_2)\rightarrow 3b_1$ transition. Their experimentally observed energies show quite large differences (Table II) for the two different polarization directions when compared to the polarization differences in the GS. If the $2b_2$ and $6e$ orbitals are almost degenerate, the observed transitions at 3.97 eV ($\mathbf{E}\|a$) and 4.36 eV ($\mathbf{E}\|c$) have to be assigned to the $(2b_2,6e)\rightarrow 3b_1$ transition, whereby the difference of about 0.4 eV can not origin in the excitation of different vibrations. All in all the observed and calculated orbital level scheme for SI show distinct differences, which does not allow an unambiguous assignment of the transitions.

TABLE III. Refined parameters to the absorption spectra of SII in single crystals of SNP at $T=100$ K.

| $\|c$ | $\nu_{max}[cm^{-1}]$ | A $[10^6 cm^{-2}]$ | $\Gamma[cm^{-1}]$ | $\tau[\mu s]$ | f $[10^{-3}]$ | $\tilde{\nu}^{exp}_{max}$[eV] | $\tilde{\nu}^{calc}_{max}$[eV] |
|---|---|---|---|---|---|---|---|
| $a''\rightarrow a'$ | $17850\pm80$ | $0.91\pm0.03$ [a] | $5450\pm100$ | 6.2 | 0.76 | 2.21 | 2.352 |
| $\|a$ | $\nu_{max}[cm^{-1}]$ | $A[10^6 cm^{-2}]$ | $\Gamma[cm^{-1}]$ | $\tau[\mu s]$ | f $[10^{-3}]$ | $\tilde{\nu}^{exp}_{max}$[eV] | $\tilde{\nu}^{calc}_{max}$[eV] |
| $a''\rightarrow a''$ | $14000\pm100$ | $0.86\pm0.05$ [b] | $3000\pm200$ | 7.5 | 1.0 | 1.74 | 1.633 |
| $a'\rightarrow a'$ | $16350\pm100$ | $2.4\pm0.2$ [b] | $4700\pm200$ | 2 | 2.8 | 2.03 | 2.066 |
| $a'\rightarrow a'$ | $22200\pm200$ | $0.6\pm0.3$ [b] | $4400\pm300$ | 4.2 | 72 | 2.75 | 2.580 |

[a]38% population.
[b]27% population.

For the polarization analysis and assignment of the transitions of SII in $C_s$ only one symmetry element is left (mirror plane perpendicular to the $c$ axis). There are only selection rules for $\mathbf{E}\|c$, where transitions $a'\rightarrow a''$ and $a''\rightarrow a'$ are allowed. For $\mathbf{E}\|a$ no selection rules apply, i.e., we may observe all possible transitions in the measured energy range. This is reflected in experiment by the fact that we observe three transitions for $\mathbf{E}\|a$ whereas for $\mathbf{E}\|c$ only one transition is found. In principle three (six) transitions would be possible for $\mathbf{E}\|c(a)$ in the energy range from 1.35 to 2.60 eV following the calculated energy splitting (Fig. 11). Therefore we suggest the assignment indicated in Table III and Figs. 9 and 11 following the calculated energy differences. For $\mathbf{E}\|c$ the highest calculated energy difference of 2.352 eV is assigned to the observed transition from the three possible transitions at 1.347, 1.861, and 2.352 eV. The assignment for $\mathbf{E}\|a$ opens even more possibilities. We assign the observed transitions to the three calculated energy differences $a''\rightarrow a''$ at 1.633 eV, $a'\rightarrow a'$ at 2.352 eV, and $a'\rightarrow a'$ at 2.580 eV, since a further $a'\rightarrow a''$ transitions would be observed also with $\mathbf{E}\|c$. For a more comprehensive assignment, calculation of matrix elements and the measurement of transition at higher energies is necessary.

In addition to the determination of the electronic structure we can also draw conclusions about the population dynamics of the metastable states from the absorption spectra: every light-induced excitation or de-excitation of GS, SI, and SII involves as an intermediate state the $\pi^*$(NO) orbital. We can excite the transitions GS$\rightarrow\pi^*$(NO)$\rightarrow$SI and GS$\rightarrow\pi^*$(NO)$\rightarrow$SII by illumination with light in the spectral region $\Delta\lambda\approx$375–562 nm. A deexcitation SI$\rightarrow$GS via $\pi^*$(NO) is not observed, since no absorption bands of SI appear between the isosbestic points. On the other hand an excitation SII$\rightarrow\pi^*$(NO)$\rightarrow$GS is possible. Following the orbital level diagrams of the DFT calculations[11] SI is always excited via SII. First the 90°-bent configuration of SII is built and afterwards the 180° inverted geometry of SI (Fe-O-N) is reached. Since we do not observe an optical deexcitation process SI$\rightarrow\pi^*$(NO)$\rightarrow$GS in the spectral range between the isosbestic points, it should be possible to transfer all anions into the metastable state SI, if just illuminating long enough in this wavelength regime. This is not observed in experiment, where a maximum population of SI of approximately 50% is found. Therefore there may be other mechanisms involved, which enable the deexcitation SI$\rightarrow$GS, provided the assumption (i.e., the inversion of the Fe-N-O to Fe-O-N) made for the DFT calculations is correct. Indicated by the isosbestic points in Fig. 8 an effective transfer SI$\rightarrow$SII via $\pi^*$(NO) is possible at wave numbers lower than 13 200 $cm^{-1}$ ($\mathbf{E}\|c$) and 11 000 $cm^{-1}$ ($\mathbf{E}\|a$), since the larger cross section for the transfer SII$\rightarrow\pi^*$(NO)$\rightarrow$GS depopulates SII for higher wave numbers. This is the reason why for illumination of SI with 9398.5 $cm^{-1}$ ($\lambda=1064$ nm) an effective population of SII of about 35% is obtained. In principle this transfer should be maximal when illuminating with a wavelength where only SI is excited, but no transition out of SII is allowed. This is possible at wavenumbers below 9000 $cm^{-1}$.

## V. CONCLUSIONS

Polarized absorption spectroscopy revealed the light-induced absorption changes in SNP caused by the excitation of the two metastable states SI and SII. The assignment of the five observed GS transitions is in agreement with earlier publications[31,33] and with the calculated orbital level diagram. Three electronic transitions are observed during the population of SI. Their tentative assignment to the calculated energy differences of the orbital level diagram under $C_{4v}$ symmetry is not unambiguous and opens the questions if the assumption, that the Fe-N-O bond is inverted to Fe-O-N, is correct.

Four electronic transitions are observed during the transfer SI$\rightarrow$SII. Their assignment to the calculated orbital level diagram yields reasonable agreement, indicating that the point symmetry of the anion in SII is indeed reduced to $C_s$.

The appearance of isosbestic points during the population process of SI indicates that single anions are excited from one state to the other. All optical excitation and deexcitation processes involve the $\pi^*$(NO) orbital as an intermediate state. An optical depopulation of SI via $\pi^*$(NO) is very unlikely in the spectral range $\Delta\lambda\approx$375–562 nm, since the absorption cross section of SI is very small or even vanishes.

Isosbestic points in the near infrared spectral range indicate that an effective transfer SI$\rightarrow$SII is possible for wavelengths $\lambda>770$ nm and $\lambda>910$ nm when illuminating with $\mathbf{E}\|c$ and $\mathbf{E}\|a$, respectively.

## ACKNOWLEDGMENTS

Financial support by the Swiss National Science Foundation (Grant No. 21-57084.99) is greatfully acknowledged.

*Electronic address: dominik.schaniel@psi.ch

[1] M. Imlau, S. Haussühl, T. Woike, R. Schieder, V. Angelov, R. Rupp, and K. Schwarz, Appl. Phys. B: Lasers Opt. **68**, 877 (1999).
[2] T. Woike, S. Haussühl, B. Sugg, R. Rupp, J. Beckers, M. Imlau, and R. Schieder, Appl. Phys. B: Lasers Opt. **63**, 243 (1996).
[3] W. Krasser, T. Woike, S. Haussühl, J. Kuhl, and A. Breitschwerdt, J. Raman Spectrosc. **17**, 83 (1986).
[4] J. Hong, P. Yeh, D. Psaltis, and D. Brady, Opt. Lett. **15**, 344 (1990).
[5] H. Zöllner, W. Krasser, T. Woike, and S. Haussühl, Chem. Phys. Lett. **161**, 497 (1989).
[6] T. Woike, H. Zöllner, W. Krasser, and S. Haussühl, Solid State Commun. **73**, 149 (1990).
[7] T. Woike and S. Haussühl, Solid State Commun. **86**, 333 (1993).
[8] K. Ookubo, Y. Morioka, H. Tomizawa, and E. Miki, J. Mol. Struct. **379**, 241 (1996).
[9] P. Coppens, D.V. Fomitchev, M.D. Carducci, and K. Culp, J. Chem. Soc. Dalton Trans. **6**, 865 (1998).
[10] D. Fomitchev, I. Novozhilova, and P. Coppens, Tetrahedron **56**, 6813 (2000).
[11] B. Delley, J. Schefer, and T. Woike, J. Chem. Phys. **107**, 10 067 (1997).
[12] S. Da Silva and D. Franco, Spectrochim. Acta, Part A **55**, 1515 (1999).
[13] S. Gorelsky and A. Lever, Int. J. Quantum Chem. **80**, 636 (2000).
[14] P. Boulet, M. Buchs, H. Chermette, C. Daul, E. Furet, F. Gilardoni, F. Rogemond, C. Schläpfer, and J. Weber, J. Phys. Chem. A **105**, 8991 (2001).
[15] P. Gütlich, Y. Garcia, and T. Woike, J. Coord. Chem. **219-221**, 839 (2001).
[16] P. Coppens, I. Novozhilova, and A. Kovalevsky, Chem. Rev. **102**, 861 (2002).
[17] H. Zöllner, T. Woike, W. Krasser, and S. Haussühl, Z. Kristallogr. **188**, 139 (1989).
[18] T. Woike, W. Krasser, H. Zöllner, W. Kirchner, and S. Haussühl, Z. Phys. D: At., Mol. Clusters **25**, 351 (1993).
[19] J. Schefer, T. Woike, M. Imlau, and B. Delley, Eur. Phys. J. B **3**, 349 (1998).
[20] M. Rüdlinger, J. Schefer, G. Chevrier, N. Furer, H. Güdel, H. Haussühl, and G. Heger, Z. Phys. B: Condens. Matter **83**, 125 (1991).
[21] J. Schefer, T. Woike, S. Haussühl, and M. Fernandez-Diaz, Z. Kristallogr. **212**, 29 (1997).
[22] M. Carducci, M. Pressprich, and P. Coppens, J. Am. Chem. Soc. **119**, 2669 (1997).
[23] P. Manoharan and W. Hamilton, Inorg. Chem. **2**, 1043 (1963).
[24] F. Bottomley and P. White, Acta Crystallogr., Sect. B: Struct. Crystallogr. Cryst. Chem. **35**, 2193 (1979).
[25] D. Schaniel, J. Schefer, B. Delley, M. Imlau, and T. Woike, in *Applications of Ferromagnetic and Optical Materials, Storage and Magnetoelectrics (Symposium V)*, edited by M. Wuttig, L. Hesselink, and H. J. Borg, MRS Spring Metting No. 674 (Materials Research Society, Warrendale, PA, 2001).
[26] A. Kaminskii, *Laser Crystals* (Springer Verlag, 1981).
[27] B. Delley, J. Chem. Phys. **92**, 508 (1990).
[28] B. Delley, J. Chem. Phys. **113**, 7756 (2000).
[29] A.D. Becke, Phys. Rev. A **38**, 3098 (1988).
[30] J. Perdew, J. Chevary, S. Vosko, K. Jackson, M. Pederson, D. Singh, and C. Fiolhais, Phys. Rev. B **46**, 6671 (1992).
[31] S. Wolfe and J. Swinehart, Inorg. Chem. **14**, 1049 (1975).
[32] O. Horvath and K. Stevenson, *Charge Transfer Photochemistry of Coordination Compounds* (VCH Publishers, New York, 1993).
[33] P. Manoharan and H. Gray, J. Am. Chem. Soc. **87**, 3340 (1965).
[34] O. Zakharieva, T. Woike, and S. Haussühl, Spectrochim. Acta, Part A **51**, 447 (1995).
[35] M. Imlau, T. Woike, R. Schieder, and R. Rupp, Phys. Rev. Lett. **82**, 2860 (1999).
[36] M. Imlau, T. Woike, D. Schaniel, J. Schefer, M. Fally, and R. Rupp (unpublished).
[37] R. Fenske and R. DeKock, Inorg. Chem. **11**, 437 (1972).
[38] M. Braga, A. Pavao, and J. Leite, Phys. Rev. B **23**, 4328 (1981).